nature neuroscience

RESOURCE

A robust and high-throughput Cre reporting and characterization system for the whole mouse brain

Linda Madisen[1], Theresa A Zwingman[1], Susan M Sunkin[1], Seung Wook Oh[1], Hatim A Zariwala[1], Hong Gu[1], Lydia L Ng[1], Richard D Palmiter[2], Michael J Hawrylycz[1], Allan R Jones[1], Ed S Lein[1] & Hongkui Zeng[1]

The Cre/lox system is widely used in mice to achieve cell-type-specific gene expression. However, a strong and universally responding system to express genes under Cre control is still lacking. We have generated a set of Cre reporter mice with strong, ubiquitous expression of fluorescent proteins of different spectra. The robust native fluorescence of these reporters enables direct visualization of fine dendritic structures and axonal projections of the labeled neurons, which is useful in mapping neuronal circuitry, imaging and tracking specific cell populations *in vivo*. Using these reporters and a high-throughput *in situ* hybridization platform, we are systematically profiling Cre-directed gene expression throughout the mouse brain in several Cre-driver lines, including new Cre lines targeting different cell types in the cortex. Our expression data are displayed in a public online database to help researchers assess the utility of various Cre-driver lines for cell-type-specific genetic manipulation.

In functional studies of the mouse brain, transgenic lines have played an invaluable role in various strategies including: labeling specific neurons by fluorescent protein expression[1–3], knocking out or overexpressing genes in specific cell types[4–6] and ablating or inhibiting activity of specific neuronal populations[7–9]. New molecular tools developed over the last decade have transformed approaches to study neural circuitry and plasticity with exquisite detail and control (reviewed in refs. 10,11). For example, use of transgenic mice that express fluorescent markers at relatively high levels in defined neuronal populations, such as *Thy1-EYFP* (ref. 1), has facilitated detailed studies of the properties of a single neuron—morphology, connectivity, electrophysiology and gene expression[2,12]—and permits long-term *in vivo* imaging[13]. The Brainbow mice introduced a new strategy for simultaneous mapping of projections and connectivity among multiple neurons using multicolored fluorescence[14]. Genetic manipulations that allow one to reversibly activate or silence neurons are powerful new ways to examine neural circuits that underlie behavior and plasticity. Among these, manipulation of neuronal activity on a millisecond scale is achievable by expression of light-gated ion channels such as channelrhodopsin (ChR2)[15].

However, a significant hurdle for widespread use of ChR2 is that high expression is required to generate sufficient current to activate target neurons. Whereas this has been achieved using acute approaches that deliver high transgene copy numbers, such as *in utero* electroporation or recombinant viruses, robust ChR2 expression has been difficult to obtain in transgenic mice, with the exception of an approach using the *Thy1* promoter[16]. However, the *Thy1* promoter is sensitive to positional effects when randomly integrated into the genome, has a postnatal onset of expression, and lacks ubiquitous neuronal expression. Like ChR2, many other genetic tools would also benefit from a strong and universal transgenic expression platform. One of the most desirable ways to achieve this is to develop universal Cre-responder lines that strongly express fluorescent markers or genetic tools.

So far, the most commonly used locus for generating Cre-responder mice is the *Gt(ROSA)26Sor* (*Rosa26*) locus[17]. However, expression of fluorescent reporters (for example, GFP) directly from the endogenous *Rosa26* promoter[18] is poor in the adult mouse brain. Other Cre-reporter lines using strong promoters but integrated into random loci (for example, Z/EG (ref. 19) and Brainbow (ref. 14) are generally not universally expressed). Thus, there remains a need for a Cre-dependent system with the potential to confer high-level responder expression in any Cre-defined cell type. Although serving different purposes, the creation of the MADM (ref. 3) and mT/mG (ref. 20) mice demonstrated a potential approach to achieving higher universal expression by incorporating a stronger exogenous promoter into a permissive genomic locus such as *Rosa26*. Furthermore, despite the widespread use of Cre lines and the importance of complete knowledge of where Cre-mediated recombination occurs, the lack of a systematic approach for Cre expression profiling has prevented full characterization of Cre-dependent gene expression patterns in many Cre-driver lines, creating uncertainty in interpretation of results and in selection of appropriate Cre lines for specific research purposes.

Here we report the development of several robust and universal Cre-responder lines that show intense native fluorescent labeling. We further introduce a public database for systematic characterization of Cre recombination patterns in various Cre-driver lines. Characterization data for 21 Cre-driver lines, including 10 newly generated Cre lines that target cortical cell types, are presented in the database. These new Cre lines could be useful tools in the study of cortical

[1]Allen Institute for Brain Science, Seattle, Washington, USA. [2]Howard Hughes Medical Institute, Department of Biochemistry, University of Washington, Seattle, Washington, USA. Correspondence should be addressed to H.Z. (hongkuiz@alleninstitute.org).

Received 21 May; accepted 6 November; published online 20 December 2009; doi:10.1038/nn.2467

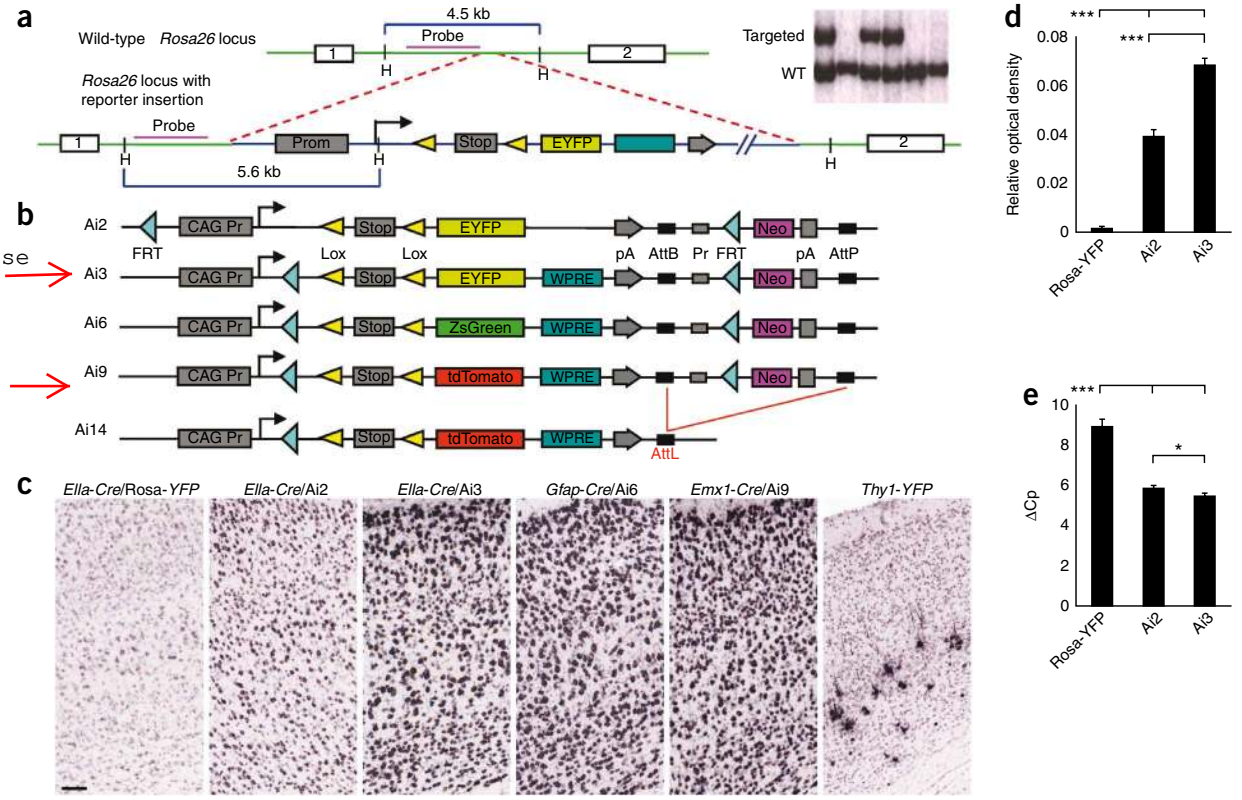

We have these

Figure 1 Generation of the Cre-reporter lines. (**a**) Schematic diagram of the gene targeting strategy to insert the Cre reporter cassette into the *Rosa26* locus, in the intron between endogenous exons 1 and 2. Right, partial Southern blot screen using HindIII-digested genomic DNA and the probe indicated in the diagram. Full-length blot in **Supplementary Figure 1**. WT, wild type. (**b**) Configurations of different Cre-reporter constructs inserted into the *Rosa26* locus. The *PGK-Neo* marker in Ai9 ES clone was deleted by transfection of a PhiC31-expressing plasmid, generating the Ai14 ES clone. (**c**) Comparison of reporter expression in the cortex between Rosa26-EYFP and new reporter lines. Cre lines used are indicated above each panel. Scale bar, 100 μm. (**d**) Quantification of *EYFP* ISH signals in *EIIa-Cre*;Rosa26-YFP, *EIIa-Cre*;Ai2 and *EIIa-Cre*;Ai3 mice with whole brain sections as AOIs. Relative optical density was measured as the IOD ratio: IOD / total AOI area. IOD = ΣOD(*p*), such that the optical densities of individual expression object pixels (*p*) are summed over the AOI. ***$P < 0.001$ ($n = 3$ sections per brain; Student's *t*-test). (**e**) Quantitative reverse transcription–PCR of *EYFP* using two sets of primer pairs on the total RNA extracted from cerebella of *Pcp2-Cre*;Rosa26-EYFP, *Pcp2-Cre*;Ai2 or *Pcp2-Cre*;Ai3 mice. ΔCp = Cp *YFP* – Cp *Gapdh*. Cp, number of real-time PCR cycles. Rosa26-YFP, $n = 4$; Ai2, $n = 8$; Ai3, $n = 12$; Student's *t*-test. ***$P < 0.001$; *$P < 0.05$. Mean ± s.e.m.

circuits and function. Through standardized and detailed anatomical profiling of transgene expression in the entire mouse brain, this data set provides a comprehensive evaluation of each transgenic mouse line to help researchers choose appropriate transgenic tools for studying the function of specific regions and/or cell types of the brain.

RESULTS

Generation of Cre-reporter mice from a universal locus

We used the *Rosa26* locus[17] to develop a universal Cre-responder because *Rosa26* is a ubiquitously expressed locus that also permits an exogenous strong promoter inserted within it to drive higher expression[3,20]. The *Rosa26* locus was modified by targeted insertion of a construct containing the strong and ubiquitously expressed *CAG* promoter, followed by a *loxP*-flanked ('floxed') stop cassette–controlled fluorescent marker gene (**Fig. 1a** and **Supplementary Fig. 1**). We generated four lines, Ai2, Ai3, Ai6 and Ai9 (**Fig. 1b**) with similar components but different fluorescent proteins: EYFP, ZsGreen or tdTomato. ZsGreen and tdTomato are among the brightest fluorescent proteins available[21]. The woodchuck hepatitis virus posttranscriptional regulatory element (*WPRE*)[22] was used in all but the Ai2 line to enhance mRNA transcript stability.

Using the pair of PhiC31 recognition sites, *AttB*/*AttP*, the *PGK-Neo* marker can be deleted from the reporter lines in either embryonic stem (ES) cells or mice (**Supplementary Fig. 2**). This was done for the Ai9 line by transfecting Ai9 ES cells with a PhiC31-expressing plasmid[23] to produce the ΔNeo line, Ai14 (**Fig. 1b**). Removal of the stop cassette by *Cre* transfection showed that both ZsGreen and tdTomato produced brighter fluorescence than EYFP in ES cells (**Supplementary Fig. 3**). In addition, we incorporated a pair of *FRT* sites to allow a Flp recombinase–mediated replacement strategy ('Flp-in') to swap other genes into the same locus at high efficiency (>90%) using a double selection strategy (**Supplementary Fig. 4**).

Strong fluorescent labeling of various brain cell types

We bred the new reporter lines with various Cre lines (**Table 1**) to test expression of the reporter genes and compare with the existing line carrying the *Rosa26-EYFP* reporter[18]. In a direct comparison at the mRNA level by *in situ* hybridization (ISH) of Cre-activated reporter gene expression in the cortex (**Fig. 1c**), the *Rosa26-EYFP* reporter line showed weak *EYFP* signal throughout the cortex. The Ai2 line expressed more *EYFP* than the *Rosa26-EYFP*, albeit still moderate amounts. The Ai3, Ai6 and Ai9 lines were similar to one another in showing strong expression of the reporter genes; reporter expression at the single-cell level in these lines approached that in the strongly expressing *Thy1-EYFP* mice[1]. We observed similar results in other brain regions in all other Cre-reporter crosses mentioned in **Table 1** (data not shown).

To quantify expression difference in ISH signals for *Rosa26-EYFP*, Ai2 and Ai3, which all used the same *EYFP* probe for ISH, relative optical density measured as the integrated optical density (IOD) ratio was computed for each area of interest (AOI) using algorithms previously developed[24]. In a comparison of mice in which each reporter line was crossed to the ubiquitously expressing *EIIa-Cre* line (using the adenovirus *EIIa* promoter), with whole brain sections as AOIs (**Fig. 1d**), the differences in expression between *Rosa26-EYFP*, Ai2 and Ai3 were highly significant ($P < 0.001$ in all pairwise comparisons). Moreover, we performed quantitative reverse transcription–PCR of *EYFP* (**Fig. 1e**) on the cerebella of mice in which each reporter line was crossed to the *Pcp2-Cre* line, which drives Purkinje cell–specific expression in the cerebellum. Amplification of *EYFP* transcript from *Rosa26-EYFP* required significantly more cycles than that from Ai2 or Ai3 (differs by >3 PCR cycles, $P < 0.001$ in both comparisons), whereas the difference between Ai2 and Ai3 was small (~0.4 PCR cycles) but still significant ($P = 0.021$).

Consistent with the ISH and quantitative PCR results, all reporter lines showed moderate (in Ai2) to strong (in Ai3, Ai6, Ai9 and Ai14) native fluorescence. In particular, Ai6, Ai9 and Ai14 showed bright fluorescence throughout the body (for example, **Supplementary Fig. 5**) that could greatly facilitate *in vivo* imaging. In the adult brains, when crossed to the same Cre line, different new reporter lines gave similar expression patterns overall with different degrees of fluorescence intensity (**Fig. 2a**,**b**), all substantially stronger than *Rosa26-EYFP*, whose native fluorescence is mostly below detection and requires immunohistochemical (IHC) staining to reveal expression. Whereas the EYFP and tdTomato fluorescence was uniformly distributed throughout the cells and their processes, the Ai6 ZsGreen fluorescence was mostly confined to cell bodies, giving rise to a punctate cellular labeling pattern (**Fig. 2a**,**b** and **Supplementary Fig. 6**).

Table 1 Cre driver lines that have been characterized

Cre line[a]	Reporter	CISH data	DFISH data	XFP data	Expression highlight[b]	JAX or MMRRC number
8030451F13Rik-Tg2-Cre	Ai9 Ai2	tdTomato, Cre	tdTomato/Gad1[d]	tdTomato EYFP	Scattered populations in the cortex and hippocampus	JAX no. 008848
A930038C07Rik-Tg4-Cre	Ai9	tdTomato, Cre	tdTomato/Gad1	tdTomato	Scattered populations enriched in layers 3/4/5	JAX no. 009616
Camk2a-Cre[38]	Ai2 Ai9	EYFP, Cre tdTomato	EYFP/Gad1 tdTomato/Gad1	EYFP tdTomato	Widespread in forebrain areas; for example, cortex, hippocampus, striatum	JAX no. 005359
Camk2a-CreERT2 (uninduced)[c]	Ai14 Ai6	tdTomato	tdTomato/Gad1	tdTomato ZsGreen	Scattered populations in cortex	
Camk2a-CreERT2 (induced)[c]	Ai14 Ai6	tdTomato	tdTomato/Gad1	tdTomato ZsGreen	Widespread in forebrain areas; for example, cortex, hippocampus, striatum	
Chat-Cre	Ai9 Ai6	tdTomato, Cre	tdTomato/Chat, tdTomato/Gad1	tdTomato ZsGreen	Cholinergic neurons	JAX no. 006410
Drd1a-Cre[39]	Ai3 Ai9	EYFP, Cre tdTomato	EYFP/Gad1, EYFP/Drd1a	EYFP tdTomato	Striatum and cortex	
Emx1-IRES-Cre[40]	Ai9	tdTomato, Cre	tdTomato/Gad1, Emx1/tdTomato	tdTomato	Widespread in cortex	JAX no. 005628
Erbb4-2A-CreERT2 (induced)[c]	Ai14	tdTomato, Cre	tdTomato/Gad1, Pvalb/tdTomato, Erbb4/tdTomato	tdTomato	Scattered interneuron populations in cortex, hippocampus	
Gfap-Cre[41]	Ai3 Ai6	EYFP ZsGreen, Cre	Gfap/EYFP Gfap/ZsGreen	 ZsGreen	Both astrocytes and widespread neuronal expression	JAX no. 004600
Ntsr1-Cre[27]	Ai3 Ai14	EYFP tdTomato	EYFP/Gad1 tdTomato/Gad1	EYFP tdTomato	Layer 6 specific	MMRRC no. 017266
Pvalb-2A-Cre	Ai14 Ai9	tdTomato tdTomato, Cre	tdTomato/Gad1, Pvalb/tdTomato tdTomato/Gad1, Pvalb/tdTomato	tdTomato tdTomato	Parvalbumin-positive interneurons and excitatory neurons in layer 5	
Pvalb-IRES-Cre[34]	Ai14 Ai9	tdTomato, Cre tdTomato	tdTomato/Gad1, Pvalb/tdTomato tdTomato/Gad1, Pvalb/tdTomato	tdTomato tdTomato	Parvalbumin-positive interneurons	JAX no. 008069
Pcp2-Cre[26]	Ai2 Ai9 Ai6 Ai3	EYFP tdTomato ZsGreen, Cre EYFP	Pcp2/EYFP Pcp2/tdTomato	EYFP tdTomato ZsGreen EYFP	Purkinje cells, scattered population of cells (glial) throughout the brain, also enriched neuronal expression in visual cortex	JAX no. 006207
Pomc-Cre[4]	Ai3 Ai9	EYFP, Cre	EYFP/Pomc1	EYFP tdTomato	POMC-positive neurons in hypothalamus, also in dentate gyrus	JAX no. 005965
Scnn1a-Tg1-Cre	Ai9	tdTomato, Cre	tdTomato/Gad1	tdTomato	Enriched in layer 4, plus scattered widespread expression	JAX no. 009111
Scnn1a-Tg2-Cre	Ai9	tdTomato, Cre	tdTomato/Gad1	tdTomato	Very sparse cells in layer 4, mostly in somatosensory area	JAX no. 009112
Scnn1a-Tg3-Cre	Ai9	tdTomato, Cre	tdTomato/Gad1	tdTomato	Layer 4 specific	JAX no. 009613
Six3-Cre[32]	Ai3 Ai9	EYFP tdTomato	EYFP/Gad1 tdTomato/Gad1	EYFP tdTomato	Enriched in layer 4, plus scattered populations in cortex, striatum	
Slc6a3-Cre[25]	Ai3 Ai9	EYFP, Cre tdTomato	EYFP/Slc6a3 Slc6a3/tdTomato	EYFP tdTomato	Dopamine neurons, plus sparse populations elsewhere	
Wfs1-Tg2-CreERT2 (induced)[c]	Ai9	tdTomato, Cre	tdTomato/Gad1	tdTomato	Enriched in layers 2/3	JAX no. 009614
Wfs1-Tg3-CreERT2 (induced)[c]	Ai9	tdTomato, Cre	tdTomato/Gad1	tdTomato	Enriched in layers 2/3 plus scattered populations in cortex	JAX no. 009103

[a]Cre lines underlined are newly generated lines. [b]Expression highlights describe only the most relevant cell populations targeted by the Cre lines, not including all the cell populations where Cre recombination occurs. [c]Induced or uninduced refers to with or without tamoxifen treatment for CreERT2-containing mice. [d]Probe pair for DFISH is shown as probe 1/probe 2.

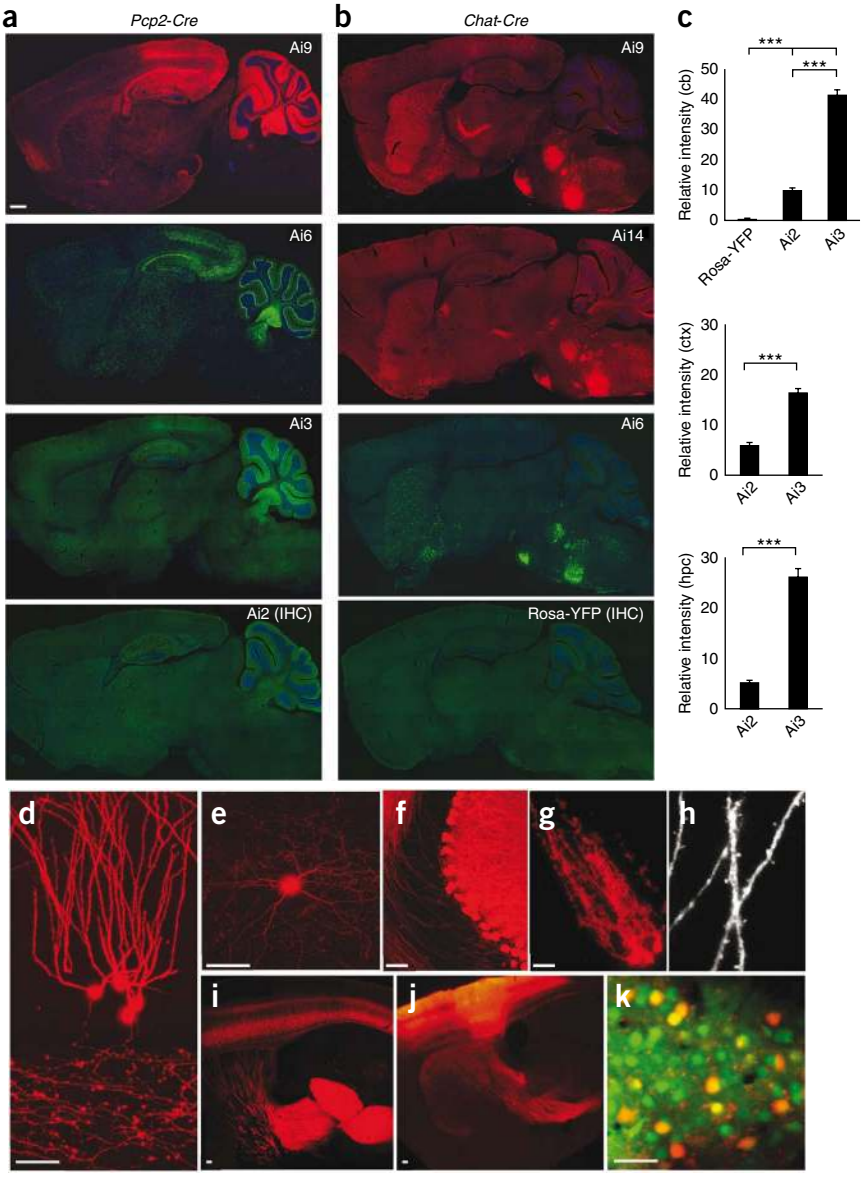

Figure 2 Significantly enhanced fluorescent labeling in the new reporter lines. (**a**,**b**) Comparison of fluorescence in various reporter lines crossed to the same Cre-driver line: *Pcp2-Cre* (**a**) and *Chat-Cre* (**b**). IHC, immunostaining using anti-GFP. Unlike tdTomato fluorescence, which was also visible in axonal projections, ZsGreen fluorescence was mostly confined to the cell bodies. Scale bar, 500 μm. (**c**) Quantification of fluorescence in single neurons of *Pcp2-Cre*;Rosa26-EYFP, *Pcp2-Cre*;Ai2 or *Pcp2-Cre*;Ai3 mice, on section images with 140-ms exposure time (no saturation). Three types of neurons were quantified: cerebellar Purkinje cells (cb, upper panel), cortical neurons (ctx, middle panel) and hippocampal CA1 pyramidal neurons (hpc, lower panel). Relative intensity = intensity of the object (cell) – intensity of the background. For each of Ai2 and Ai3, $n = 30$ randomly selected neurons from three sections per region. For Rosa26-YFP, only $n = 10$ randomly selected neurons from one section in the Purkinje cell quantification, owing to undetectability in the other two. $^{***}P < 0.001$. Mean ± s.e.m. (**d–h**) Distinctive morphologies of various cell types labeled by tdTomato: (**d**) dentate granule cells; (**e**) a cortical interneuron; (**f**) Purkinje cells; (**g**) cerebellar Bergmann glia cells; (**h**) dendritic spines. (**i**) Corticothalamic projections from cortical layer 6 neurons in *Ntsr1-Cre*;Ai14 mice. (**j**) Corticothalamic projections in an Ai14 mouse with rAAV-Cre injected into the somatosensory cortex. (**k**) *In vivo* two-photon imaging of tdTomato expressing neurons (red) and OGB-loaded neurons (green) in visual cortical layer 2/3 of an anesthetized *Wfs1-Tg2-CreERT2*;Ai9 mouse. Small red dots are dendrites crossing the imaging plane. Scale bar, 50 μm.

To assess the fluorescence intensity of different fluorescent proteins in a more objective way, we spread TetraSpeck fluorescent beads (4.0 μm) directly onto sections and used them as a standard to compare the brightness of fluorescently labeled cells in different brain sections (**Supplementary Fig. 7**). The assessed strength of native fluorescence was ranked in the following order: Rosa26-EYFP < Ai2 (EYFP) < Ai3 (EYFP) < Ai9 (tdTomato) = Ai14 (tdTomato) < Ai6 (ZsGreen), regardless of which Cre lines were used. We further quantified fluorescent signals at single-cell level (**Fig. 2c**) on sections from mice in which each of Rosa26-EYFP, Ai2 or Ai3 was crossed to *Pcp2-Cre*, which not only induces recombination in Purkinje cells but also partially elsewhere, especially in hippocampus and visual cortex. The cerebellar Purkinje cells, cortical neurons and hippocampal CA1 pyramidal cells all showed significantly stronger labeling by Ai3 than Ai2 ($P < 0.001$ in all comparisons), and labeling in Rosa26-EYFP was essentially undetectable. Taken together, these data demonstrate that the new reporter lines have enhanced reporter gene expression and there is a further improvement from Ai2 to Ai3. Difference between Ai2 and Ai3 indicates that the WPRE sequence improved transcript and/or protein expression in our system.

With the significantly enhanced reporter expression, more recombined cells than expected from previous reports were readily detected in various Cre-driver lines, such as *Slc6a3-Cre* (ref. 25) and *Pcp2-Cre* (ref. 26) (**Supplementary Fig. 8**), in which Cre-mediated recombination was previously thought to be limited to certain cell types on the basis of results in *Rosa26-lacZ* or *Rosa26-EYFP* reporter mice. These results indicate either that the new reporter lines are more sensitive to low levels of Cre, leading to a more thorough identification of Cre-positive populations, and/or that Cre-mediated recombination had occurred in more cells in previous reporter lines, but it was undetected owing to low reporter expression.

Strong tdTomato native fluorescence in Ai9 and Ai14 allowed direct visualization of fine structural details, such as dendritic spines and thin axons, of diverse cell types (excitatory, inhibitory or glial) under confocal microscopy (**Fig. 2d–h**). Further, it is possible to use these reporter lines to map long-range axonal projections. For example, breeding Ai14 to the *Ntsr1-Cre* line, known to label cortical layer 6 excitatory neurons[27], resulted in strong labeling of the corticothalamic projections (**Fig. 2i**). A Cre-expressing recombinant adeno-associated virus (rAAV-Cre) was also used in conjunction with these reporter lines to map axonal projections. Following rAAV-Cre virus injection into the somatosensory cortex of an Ai14 mouse, the

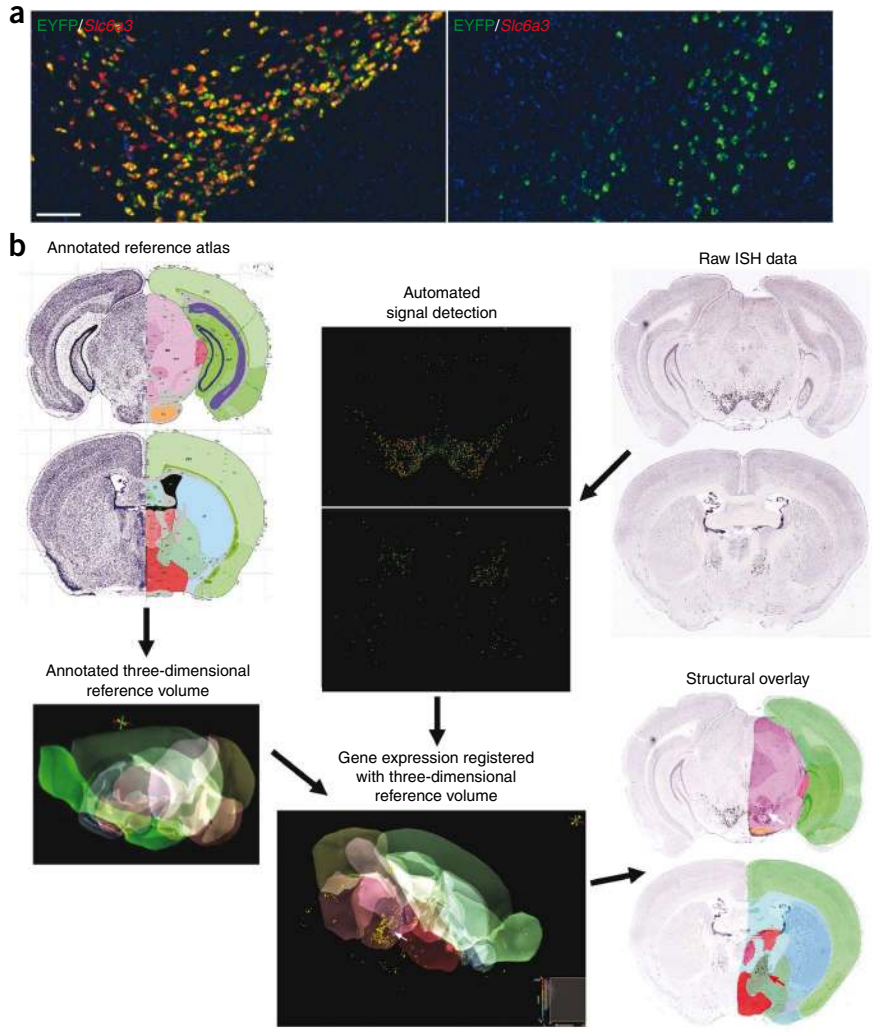

Figure 3 Informatics processing of the ISH characterization data. (**a**) Co-labeling of *EYFP* (green) with *Slc6a3* (red) in the *Slc6a3-Cre*;Ai3 mouse by DFISH. In the VTA/substantia nigra region (left panel), *EYFP* was largely colocalized with *Slc6a3* (>90% cells were co-labeled), demonstrating expected Cre recombination in dopamine neurons. In the basal forebrain area (right panel), the cluster of *EYFP*-positive cells were *Slc6a3*-negative. Scale bar, 200 µm. (**b**) *EYFP* ISH data from a *Slc6a3-Cre*;Ai3 mouse were digitized and registered to the Allen Reference Atlas, which allows anatomical search and comparison. Two sections of registered *EYFP* ISH data are shown overlaid with anatomical partitioning. *EYFP* expression is present in both sections (white and red arrows).

corticothalamic, corticocallosal and corticospinal projections were all strongly fluorescent (**Fig. 2j** and data not shown). Strong tdTomato native fluorescence also enabled direct visualization of cells in live animals by *in vivo* two-photon imaging, in which tdTomato-positive neurons (red) and calcium dye-loaded neurons (green) were easily distinguishable (**Fig. 2k**). Dendrites of tdTomato-positive neurons were also clearly visible.

Systematic characterization of Cre recombination patterns

Using the systems developed for the generation of the Allen Mouse Brain Atlas (http://mouse.brain-map.org/)[24], a characterization pipeline has been developed to systematically evaluate gene expression patterns throughout the entire mouse brain that are defined by various Cre-driver lines. The pipeline is advantageous in that characterization data are generated on sections covering the entire brain, high resolution images are obtained, ISH data are registered to the Allen Reference Atlas[28] and can be used for informatics data mining, and all characterization data are publicly displayed at http://transgenic-mouse.alleninstitute.org/.

So far, we have systematically characterized over 20 Cre-driver lines (**Table 1**). These cover both a representative set of Cre lines previously generated by other researchers for which comprehensive characterization is reported for the first time here, as well as a set of new Cre lines generated by us. The following types of data are included: (i) Colorimetric ISH (CISH) of *Cre* or the reporter gene shows mRNA expression at single-cell resolution. (ii) Double fluorescent *in situ* hybridization (DFISH) of the reporter gene with another gene of interest, either the original targeted gene or another cell-type marker, shows the degree of pattern recapitulation or the cell-type identity. (iii) XFP native fluorescence or IHC of the reporter gene shows expression of the reporter gene at the protein level throughout the brain (for example, **Fig. 2a**,**b**). A characterization example is shown in **Supplementary Fig. 9** for *Chat-Cre*.

Using previously developed algorithms for informatics image processing[29], the ISH data set can provide additional information on the localization of gene expression. As an example, we evaluated EYFP expression pattern in the *Slc6a3-Cre*;Ai3 mouse. In *Slc6a3-Cre* (ref. 25), Cre is targeted to the dopamine transporter gene (*Slc6a3*) which is expressed in dopaminergic neurons. Compared with the ISH of *Slc6a3* gene itself, EYFP expression was found to be more widespread, present not only in the dopaminergic neurons—for example, in the ventral tegmental area (VTA) and substantia nigra and colocalized with *Slc6a3* (**Fig. 3a**, left)—but present also in other brain regions, mostly sparsely scattered but also clustered in some areas of the basal forebrain (for example, **Fig. 3a**, right), corticoamygdala area and brainstem (data not shown). Registration of the EYFP ISH data to the Allen Reference Atlas was done (**Fig. 3b**), in which each section was fit into the three-dimensional reference volume along with detected ISH signals. The expression pattern was further visualized as a three-dimensional model using Brain Explorer[30], and anatomical partitioning was overlaid onto each section. The nearest Allen Reference Atlas plane was then extracted for each section to assist in the identification of the region of interest. Using this approach, the cluster of EYFP-positive cells seen in the basal forebrain was localized to the bed nuclei of the stria terminalis (**Fig. 3b**, red arrow). This prediction is consistent with previous studies indicating that the dopamine transporter might be transiently expressed in these nuclei during development[31].

Generation and characterization of new Cre-driver lines

We have generated a set of new Cre-driver lines designed to target different excitatory or inhibitory cell types in the cortex. Analysis of

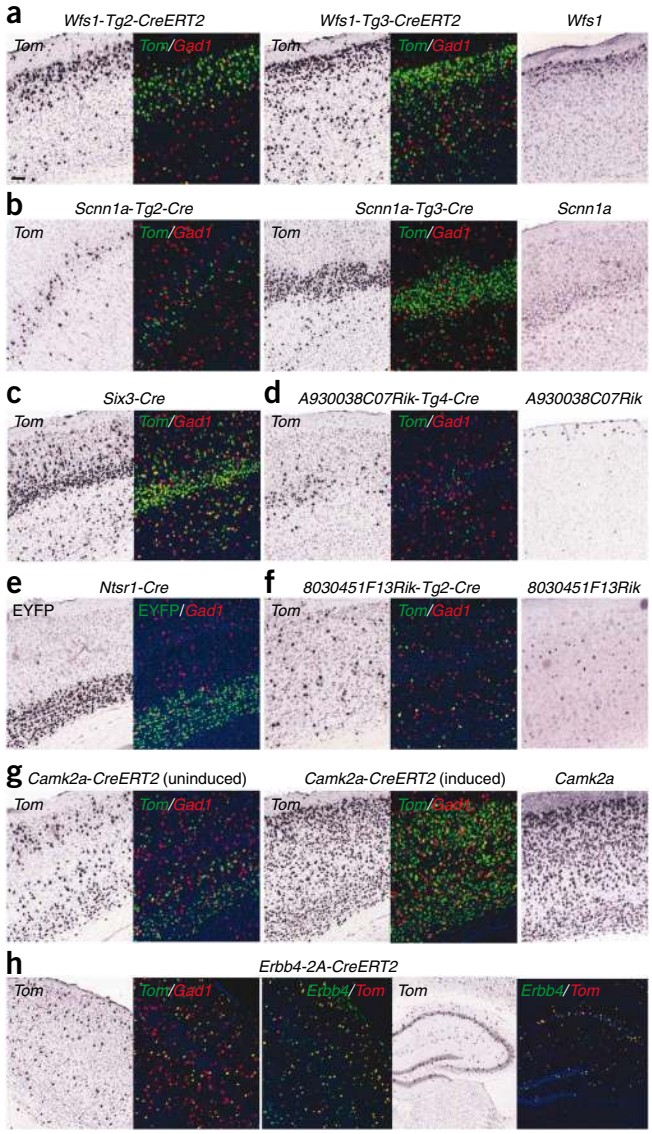

Figure 4 New Cre lines and their differential recombination patterns in different cortical cell types. For each Cre line, both CISH of the reporter gene (tdTomato (*Tom*) or *EYFP*) and DFISH of the reporter (green) with *Gad1* (red) are shown for the cortex only. Far right, CISH of some of the endogenous genes used to make Cre lines. (**a**) *Wfs1-Tg2-CreERT2*;Ai9 and *Wfs1-Tg3-CreERT2*;Ai9 with tamoxifen induction. (**b**) *Scnn1a-Tg2-Cre*;Ai9 and *Scnn1a-Tg3-Cre*;Ai9. (**c**) *Six3-Cre*;Ai9. (**d**) *A930038C07Rik-Tg4-Cre*;Ai9. (**e**) *Ntsr1-Cre*;Ai3. (**f**) *8030451F13Rik-Tg2-Cre*;Ai9. (**g**) *Camk2a-CreERT2*;Ai14 without or with tamoxifen induction. (**h**) *Erbb4-2A-CreERT2*;Ai14 with tamoxifen induction, shown for both cortex and hippocampus to demonstrate the scattered population of interneurons. DFISH of *Erbb4* (green) with tdTomato (red) shows the faithful but incomplete recapitulation of recombination in *Erbb4*-positive cells. DAPI, blue. Scale bar, 100 μm.

Cre-directed reporter expression and reporter colocalization with *Gad1* in these new Cre lines, along with two preexisting Cre lines (*Six3-Cre* (ref. 32) and *Ntsr1-Cre* (ref. 27)), illustrates diverse cortical Cre recombination patterns (**Fig. 4**). Specifically, two BAC transgenic Cre lines targeting a layer 2 marker (*Wfs1*), *Wfs1-Tg2-CreERT2* and *Wfs1-Tg3-CreERT2*, drove preferential recombination in layers 2/3 after tamoxifen induction, with somewhat different profiles (**Fig. 4a**). Two BAC transgenic Cre lines targeting a layer 4 marker (*Scnn1a*) also showed specific recombination in layer 4 of varying degrees, with very sparsely labeled layer 4 cells (mostly in the somatosensory cortex) in the *Scnn1a-Tg2-Cre* line and denser layer 4 labeling in the *Scnn1a-Tg3-Cre* line (**Fig. 4b**). In contrast to these lines, in which Cre recombination more or less followed that of the endogenous targeted genes, the following two BAC Cre lines showed patterns entirely different from those of the original genes. The *A930038C07Rik-Tg4-Cre* line showed expression in a sparse population of cells encompassing layers 3/4/5 (**Fig. 4d**), whereas the endogenous *A930038C07Rik* gene is layer 1 specific. The *8030451F13Rik-Tg2-Cre* line showed expression in a scattered population of cells that are not GABAergic (**Fig. 4f**), whereas the endogenous *8030451F13Rik* gene expresses in a scattered interneuron population. In other cases, as reported previously[27,32], the *Six3-Cre* line drove preferential expression in layer 4 (**Fig. 4c**), and the *Ntsr1-Cre* line showed specific expression in layer 6 (**Fig. 4e**). A new Cre line driven by a short (1.3 kb) *Camk2a* promoter, *Camk2a-CreERT2* (**Fig. 4g**), produced by random integration into the genome, drove 'leaky' expression in scattered excitatory neuronal populations in the uninduced state. After tamoxifen induction, expression was seen in most excitatory neurons, consistent with the endogenous *Camk2a* expression pattern. Finally, an *Erbb4-2A-CreERT2* knock-in Cre line (**Fig. 4h**), in which the *2A-CreERT2* sequence was inserted in frame to the 3′ end of the coding sequence (immediately upstream of the stop codon) of *Erbb4*, which is predominantly expressed in interneurons, showed Cre recombination in a subpopulation of GABAergic interneurons in both cortex and hippocampus only after tamoxifen induction. The reporter-labeled cells colocalized with most, but not all, cells that were *Erbb4* positive. Overall, the diversity of recombination directed by these Cre-driver lines constitutes useful tools for the study of different excitatory and inhibitory cortical cell types.

To explore the utility of the 2A sequences[33] in mediating bicistronic translation in a mechanism different from, and potentially more efficient than, the well described IRES (internal ribosome entry site) sequence, we generated a *Pvalb-2A-Cre* knock-in line, in which the *2A-Cre* sequence is inserted in frame to the 3′ end of the *Pvalb* coding sequence (immediately upstream of the stop codon). The resulting Cre-driver line has a similar genomic configuration as the previously reported *Pvalb-IRES-Cre* line[34], in which *IRES-Cre* is inserted by knock-in into the *Pvalb* 3′ untranslated region. A comparison of Ai14 reporter expression in crosses to each of the two *Pvalb* Cre-driver lines is shown in **Figure 5**. *Pvalb* is a robust marker for a subset of cortical interneurons (for example, basket cells and chandelier cells), but it was also expressed at lower levels in other types of cells—for example, some layer 5 pyramidal neurons (**Fig. 5b**). In thalamus, *Pvalb* was expressed most strongly in the reticular nucleus and less strongly in other regions, such as the ventral posteromedial nucleus (**Fig. 5h**). We found that, in the *Pvalb-IRES-Cre* mice, recombination seemed to occur only in cells with strongest *Pvalb* expression; that is, those large interneurons, and thus a more restricted (and perhaps more specific) pattern emerged than that of the *Pvalb* gene itself. By contrast, in the *Pvalb-2A-Cre* mice, recombination seemed to be more widespread, occurring in cells with both high and low *Pvalb* expression. These results indicate that different recombination patterns may be produced from different targeting methods even in the same locus. An IRES-mediated approach may result in lower Cre protein levels and may be better used in conjunction with strong genes to increase recombination specificity. A 2A-based approach may produce more equimolar amounts of Cre relative to the targated gene and may be better used with weakly expressing genes to increase sensitivity. Our

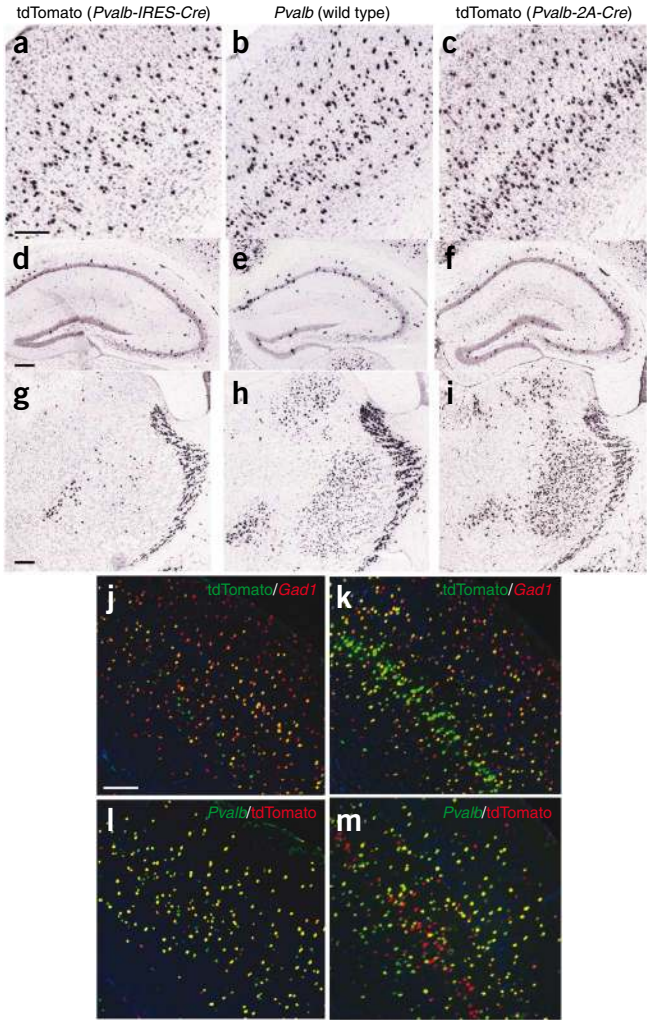

Figure 5 Comparison of recombination patterns in two closely related knock-in Cre lines, *Pvalb-IRES-Cre* and *Pvalb-2A-Cre*. (**a**–**i**) CISH comparison of tdTomato reporter in *Pvalb-IRES-Cre*;Ai14 mouse (**a**,**d**,**g**), the endogenous *Pvalb* gene (**b**,**e**,**h**) and tdTomato reporter in *Pvalb-2A-Cre*; Ai14 mouse (**c**,**f**,**i**) in three areas of the brain: cortex (**a**–**c**), hippocampus (**d**–**f**) and thalamus (**g**–**i**). (**j**,**k**) DFISH comparison of tdTomato (green) with Gad1 (red) between *Pvalb-IRES-Cre* (**j**) and *Pvalb-2A-Cre* (**k**). (**l**,**m**) DFISH comparison of Pvalb (green) with tdTomato (red) between *Pvalb-IRES-Cre* (**l**) and *Pvalb-2A-Cre* (**m**). Scale bar, 200 μm.

data suggest a source of recombination variability beyond the commonly recognized positional effect as seen in the above BAC Cre lines. Also, to our knowledge, the *Pvalb-2A-Cre* and *Erbb4-2A-CreERT2* are the first demonstration that 2A sequences are able to mediate faithful Cre expression when targeted to the endogenous gene loci.

DISCUSSION

Given the potential of using transgenic tools to tease out different components of complex neural circuits, great effort has been put into developing many cell type–specific Cre-driver lines (for example, ref. 27). The field is just beginning to create the necessary number of Cre-responsive lines expressing molecular probes or tools. Impeding successful development of useful lines is the requirement for most of these probes or tools to be expressed at sufficiently high levels for them to work well *in vivo*; so far, there has not been an optimal way to achieve this expression. Cre-responding recombinant viral vectors can confer strong expression, and they offer a fast, convenient alternative approach[35,36]. However, variability among viral stocks, serotypes, injected animals, cell-type infection efficiency, number of viral particles present in individual cells, and so forth is inherent to the viral approach, and is a major issue in functional studies. Here, we demonstrate success in creating a consistent and versatile system to strongly express fluorescent probes. Notably, our system should allow us to express various additional functional genes, which in combination with the ever increasing number of Cre mouse lines will expand the arsenal of Cre-controlled tools specific for a variety of cell types.

The expression of exogenous genes at high levels always carries the risk of potential toxicity. So far we have not observed any morphological abnormalities in either the mice or the various cell types examined. Notably, we have created animals of which the floxed stop cassette is deleted in germline and the fluorescent reporters are strongly expressed throughout the body. These animals are healthy and fertile, with no significant behavioral or anatomical abnormalities. Nonetheless, it will be necessary to continue monitoring for potential subtle phenotypes.

In addition to what we have shown, one can envision more applications in the use of these new Cre-reporter lines, especially the Ai9 and Ai14 tdTomato lines. Upon crossing to different cell type–specific Cre lines, one can examine the morphology of labeled cells, trace axonal projections (in a way similar to ref. 37), record electrophysiological activities, perform short-term and long-term *in vivo* imaging, and follow development and differentiation. Specific cell populations can also be isolated by cell sorting or other means for subsequent gene expression profiling, culturing or transplantation. Cell types with distinguishable fluorescent labels can be mixed or transplanted together to examine their interactions and formation of microcircuits both *in vitro* and *in vivo*.

Through the systematic analysis of various Cre-driver lines, we observed a wide range of Cre recombination patterns that could be less than, more than, or different from what was expected. This diversity could be due to positional effect of a randomly integrated Cre-transgene, the level of Cre expression, the accessibility of floxed targets, or early developmental or sporadic, transient expression of Cre. The latter could also be a faithful reflection of the developmental or transient expression of the original targeted gene in previously unknown cell types, thus it could serve to uncover new functions of the gene. So far, we have characterized only adult mouse brains. It will be useful to expand these characterizations into different developmental stages as well as other tissues. Since Cre recombination converts dynamic gene expression into a permanent on or off state (of a reporter or a floxed gene), this approach of collecting data in an extensive and standardized way should be valuable in guiding the choice and evaluation of different Cre transgenic tools, as well as future efforts toward using combinatorial strategies to achieve even greater cell-type-specific genetic control.

All research materials and data are publicly available. DNA constructs will be deposited to Addgene, Inc., a plasmid repository, for distribution. New Cre-reporter mice have been deposited to the JAX Mice repository for distribution (JAX Mice stock numbers: Ai2, 007920; Ai3, 007903; Ai6, 007906; Ai9, 007909; Ai14, 007914). Some of the new Cre-driver lines have also been deposited to JAX Mice (see **Table 1**), and the remaining lines are in the process. Characterization data for transgenic mice, as well as detailed experimental protocols, are available at http://transgenicmouse.alleninstitute.org/. In the future, we will continue to characterize new Cre-driver lines made by ourselves and from the scientific community, including

those that are in the JAX Mice repository. These characterization data will also be publicly available on the website.

METHODS

Methods and any associated references are available in the online version of the paper at http://www.nature.com/natureneuroscience/.

Note: Supplementary information is available on the Nature Neuroscience website.

ACKNOWLEDGMENTS

We are grateful for the professional support of the entire Atlas production team, led by P. Wohnoutka, and the Information Technology team, led by C. Dang, at the Allen Institute, without which the work would have not been possible to accomplish. We are thankful to A. Bernard for her contribution in establishing the DFISH process, L. Kuan for ISH data quantification and R. Hunter for coordinating transgenic mice production. We also gratefully acknowledge the following researchers for providing various research materials: R. Tsien (University of California at San Diego) for the tdTomato DNA construct, L. Luo (Stanford University) for the Rosa-CAG targeting construct, K. Deisseroth (Stanford University) for the WPRE-containing DNA construct, B. Sauer (National Institute of Diabetes and Digestive and Kidney Diseases) via Addgene for the Cre and EGFP-Cre DNA constructs, P. Chambon (Institut de Génétique et de Biologie Moléculaire et Cellulaire) for the CreERT2 DNA construct, P. Soriano (Fred Hutchinson Cancer Research Center) via Addgene for the PhiC31o, FLPo and pPGKneotpAlox2 DNA constructs, A. Nagy (Mount Sinai Hospital in Toronto) for the G4 ES cell line, G. Oliver (St. Jude's Children's Research Hospital) for the *Six3-Cre* mice, N. Heintz (Rockefeller University) via Mutant Mouse Regional Resource Centers (MMRRC) for the *Ntsr1-Cre* mice and X. Zhuang (University of Chicago) for the *Slc6a3-Cre* mice. The authors thank the Allen Institute founders, P.G. Allen and J. Patton, for their vision, encouragement and support. This work was funded by the Allen Institute for Brain Science and a US National Institutes of Health grant (MH085500) to H.Z.

AUTHOR CONTRIBUTIONS

H.Z. designed the study, analyzed data and wrote the paper. L.M. generated the Cre reporter lines and the knock-in Cre driver lines. T.A.Z. and E.S.L. designed and generated the BAC transgenic Cre driver lines. H.Z., S.M.S. and T.A.Z. set up the characterization pipeline and database. S.W.O. produced and performed experiments with rAAVs. H.A.Z. performed *in vivo* two-photon imaging experiments. M.J.H. and L.L.N. conducted informatics analysis. H.G. assisted with transgenic mice production and characterization. R.D.P. provided lab resources and scientific advice. A.R.J. provided institutional support.

Published online at http://www.nature.com/natureneuroscience/.
Reprints and permissions information is available online at http://www.nature.com/reprintsandpermissions/.

1. Feng, G. *et al.* Imaging neuronal subsets in transgenic mice expressing multiple spectral variants of GFP. *Neuron* **28**, 41–51 (2000).
2. Sugino, K. *et al.* Molecular taxonomy of major neuronal classes in the adult mouse forebrain. *Nat. Neurosci.* **9**, 99–107 (2006).
3. Zong, H., Espinosa, J.S., Su, H.H., Muzumdar, M.D. & Luo, L. Mosaic analysis with double markers in mice. *Cell* **121**, 479–492 (2005).
4. Balthasar, N. *et al.* Leptin receptor signaling in POMC neurons is required for normal body weight homeostasis. *Neuron* **42**, 983–991 (2004).
5. Kellendonk, C. *et al.* Transient and selective overexpression of dopamine D2 receptors in the striatum causes persistent abnormalities in prefrontal cortex functioning. *Neuron* **49**, 603–615 (2006).
6. McHugh, T.J. *et al.* Dentate gyrus NMDA receptors mediate rapid pattern separation in the hippocampal network. *Science* **317**, 94–99 (2007).
7. Karpova, A.Y., Tervo, D.G., Gray, N.W. & Svoboda, K. Rapid and reversible chemical inactivation of synaptic transmission in genetically targeted neurons. *Neuron* **48**, 727–735 (2005).
8. Luquet, S., Perez, F.A., Hnasko, T.S. & Palmiter, R.D. NPY/AgRP neurons are essential for feeding in adult mice but can be ablated in neonates. *Science* **310**, 683–685 (2005).
9. Nakashiba, T., Young, J.Z., McHugh, T.J., Buhl, D.L. & Tonegawa, S. Transgenic inhibition of synaptic transmission reveals role of CA3 output in hippocampal learning. *Science* **319**, 1260–1264 (2008).
10. Barth, A.L. Visualizing circuits and systems using transgenic reporters of neural activity. *Curr. Opin. Neurobiol.* **17**, 567–571 (2007).
11. Luo, L., Callaway, E.M. & Svoboda, K. Genetic dissection of neural circuits. *Neuron* **57**, 634–660 (2008).
12. Xu, X., Roby, K.D. & Callaway, E.M. Mouse cortical inhibitory neuron type that coexpresses somatostatin and calretinin. *J. Comp. Neurol.* **499**, 144–160 (2006).
13. Holtmaat, A., Wilbrecht, L., Knott, G.W., Welker, E. & Svoboda, K. Experience-dependent and cell-type-specific spine growth in the neocortex. *Nature* **441**, 979–983 (2006).
14. Livet, J. *et al.* Transgenic strategies for combinatorial expression of fluorescent proteins in the nervous system. *Nature* **450**, 56–62 (2007).
15. Boyden, E.S., Zhang, F., Bamberg, E., Nagel, G. & Deisseroth, K. Millisecond-timescale, genetically targeted optical control of neural activity. *Nat. Neurosci.* **8**, 1263–1268 (2005).
16. Arenkiel, B.R. *et al. In vivo* light-induced activation of neural circuitry in transgenic mice expressing channelrhodopsin-2. *Neuron* **54**, 205–218 (2007).
17. Soriano, P. Generalized *lacZ* expression with the ROSA26 Cre reporter strain. *Nat. Genet.* **21**, 70–71 (1999).
18. Srinivas, S. *et al.* Cre reporter strains produced by targeted insertion of EYFP and ECFP into the ROSA26 locus. *BMC Dev. Biol.* **1**, 4 (2001).
19. Novak, A., Guo, C., Yang, W., Nagy, A. & Lobe, C.G. Z/EG, a double reporter mouse line that expresses enhanced green fluorescent protein upon Cre-mediated excision. *Genesis* **28**, 147–155 (2000).
20. Muzumdar, M.D., Tasic, B., Miyamichi, K., Li, L. & Luo, L. A global double-fluorescent Cre reporter mouse. *Genesis* **45**, 593–605 (2007).
21. Shaner, N.C., Patterson, G.H. & Davidson, M.W. Advances in fluorescent protein technology. *J. Cell Sci.* **120**, 4247–4260 (2007).
22. Zufferey, R., Donello, J.E., Trono, D. & Hope, T.J. Woodchuck hepatitis virus posttranscriptional regulatory element enhances expression of transgenes delivered by retroviral vectors. *J. Virol.* **73**, 2886–2892 (1999).
23. Raymond, C.S. & Soriano, P. High-efficiency FLP and PhiC31 site-specific recombination in mammalian cells. *PLoS ONE* **2**, e162 (2007).
24. Lein, E.S. *et al.* Genome-wide atlas of gene expression in the adult mouse brain. *Nature* **445**, 168–176 (2007).
25. Zhuang, X., Masson, J., Gingrich, J.A., Rayport, S. & Hen, R. Targeted gene expression in dopamine and serotonin neurons of the mouse brain. *J. Neurosci. Methods* **143**, 27–32 (2005).
26. Lewis, P.M., Gritli-Linde, A., Smeyne, R., Kottmann, A. & McMahon, A.P. Sonic hedgehog signaling is required for expansion of granule neuron precursors and patterning of the mouse cerebellum. *Dev. Biol.* **270**, 393–410 (2004).
27. Gong, S. *et al.* Targeting Cre recombinase to specific neuron populations with bacterial artificial chromosome constructs. *J. Neurosci.* **27**, 9817–9823 (2007).
28. Dong, H.W. *The Allen Reference Atlas: A Digital Color Brain Atlas of the C57BL/6J Male Mouse* (Wiley, Hoboken, New Jersey, USA, 2008).
29. Ng, L. *et al.* Neuroinformatics for genome-wide 3D gene expression mapping in the mouse brain. *IEEE/ACM Trans. Comput. Biol. Bioinform.* **4**, 382–393 (2007).
30. Lau, C. *et al.* Exploration and visualization of gene expression with neuroanatomy in the adult mouse brain. *BMC Bioinformatics* **9**, 153 (2008).
31. Coulter, C.L., Happe, H.K. & Murrin, L.C. Postnatal development of the dopamine transporter: a quantitative autoradiographic study. *Brain Res. Dev. Brain Res.* **92**, 172–181 (1996).
32. Furuta, Y., Lagutin, O., Hogan, B.L. & Oliver, G.C. Retina- and ventral forebrain-specific Cre recombinase activity in transgenic mice. *Genesis* **26**, 130–132 (2000).
33. Szymczak, A.L. *et al.* Correction of multi-gene deficiency *in vivo* using a single 'self-cleaving' 2A peptide-based retroviral vector. *Nat. Biotechnol.* **22**, 589–594 (2004).
34. Hippenmeyer, S. *et al.* A developmental switch in the response of DRG neurons to ETS transcription factor signaling. *PLoS Biol.* **3**, e159 (2005).
35. Atasoy, D., Aponte, Y., Su, H.H. & Sternson, S.M.A. FLEX switch targets Channelrhodopsin-2 to multiple cell types for imaging and long-range circuit mapping. *J. Neurosci.* **28**, 7025–7030 (2008).
36. Kuhlman, S.J. & Huang, Z.J. High-resolution labeling and functional manipulation of specific neuron types in mouse brain by Cre-activated viral gene expression. *PLoS ONE* **3**, e2005 (2008).
37. Rotolo, T., Smallwood, P.M., Williams, J. & Nathans, J. Genetically-directed, cell type-specific sparse labeling for the analysis of neuronal morphology. *PLoS ONE* **3**, e4099 (2008).
38. Tsien, J.Z. *et al.* Subregion- and cell type-restricted gene knockout in mouse brain. *Cell* **87**, 1317–1326 (1996).
39. Heusner, C.L., Beutler, L.R., Houser, C.R. & Palmiter, R.D. Deletion of GAD67 in dopamine receptor-1 expressing cells causes specific motor deficits. *Genesis* **46**, 357–367 (2008).
40. Gorski, J.A. *et al.* Cortical excitatory neurons and glia, but not GABAergic neurons, are produced in the Emx1-expressing lineage. *J. Neurosci.* **22**, 6309–6314 (2002).
41. Zhuo, L. *et al.* hGFAP-cre transgenic mice for manipulation of glial and neuronal function *in vivo*. *Genesis* **31**, 85–94 (2001).

ONLINE METHODS

Gene targeting in ES cells and generation of knock-in mice. Targeting constructs were generated using a combined gene synthesis (GenScript) and molecular cloning approach. Briefly, to target the Rosa26 locus, a cassette containing the following components was constructed: *FRT* – *LoxP* – stop codons – three SV40 poly(A) sequences – *LoxP* – *EYFP* – *WPRE* – *bGH* poly(A) – *AttB* – *PGK* promoter – *FRT* – *Neo* – *PGK* poly(A) – *AttP*. For most targeting vectors, this cassette was cloned into a Rosa-CAG targeting vector[3], downstream of the *CAG* promoter and upstream of the 3′ arm, to generate the final EYFP targeting vector. Unique restriction sites flanking the *EYFP* gene were used to replace *EYFP* with alternative reporter genes. For the Ai2 vector, which lacks the WPRE, the *CAG* promoter was inserted between the first *FRT* and *LoxP* sites, and the cassette was cloned immediately downstream of the 5′ homology arm. The final targeting vectors contained 5′ and 3′ homology arms of 1.1 kb and 4.3 kb, as well as a *PGK-DTA* cassette for negative selection. Targeting constructs for knock-in Cre lines inserted into other gene loci were constructed in similar ways.

The targeting vectors were linearized and transfected into the 129/B6 F1 hybrid ES cell line G4 (ref. 42) using an Amaxa electroporator. G418-resistant ES clones were screened by Southern blot analysis of HindIII digested DNA, which was probed with a 1.1-kb genomic fragment from immediately upstream of the 5′ arm. We observed a recombination rate of about 25% for the four constructs. Positive ES cell clones were injected into C57BL/6J blastocysts to obtain chimeric mice following standard procedures. Both ES cell transfections and blastocyst injections were performed by the University of Washington Transgenic Resources Program. Because of the robustness of the G4 cells, we routinely obtained high-percentage chimeras and high rates of germline transmission. Chimeric mice were bred with either C57BL/6J mice to obtain germline transmission or various Cre-driver lines for direct characterization.

An Ai9 ES cell clone with strong germline transmission potency was used in subsequent transfections for the Flp-mediated exchange strategy outlined in **Supplementary Figure 4**. Ai9 ES cells were transfected using a Bio-Rad electroporator with 100 μg of pCAGGS-FLPe (Open Biosystems) and 40 μg of an incoming replacement vector. After 8–10 d of Hygromycin B selection, surviving colonies that also appeared green by fluorescence microscopy were picked and screened by PCR using primer sets designed to confirm a correct insertion of the incoming vector at the 5′ and 3′ *FRT* recombinase sites.

Generation of BAC transgenic Cre-driver lines. Plasmids containing straight *Cre* and inducible *CreERT2* along with a selectable marker flanked by *FRT* sites (*FRT-Neo-FRT*) were used for all subsequent targeting to BACs containing genes of interest. The *Cre FRT-Neo-FRT* portions of the plasmids were PCR-amplified with flanking oligonucleotides that were designed to have 50-bp homology arms with the BAC of interest. Specific BAC clones were RP23-476E22 for *A930038C07Rik*, RP23-405O19 for *Wfs1*, RP23-405B24 for *Scnn1a*, and RP23-116K19 for *8030451F13Rik*. RedET recombination[43] was used to insert the sequence verified PCR product into the ATG start site of the specific gene locus on each BAC. Flp recombination was used to remove the neomycin selection marker from the BAC. The wild-type *loxP* site present in the RP23 BAC backbone was removed before pronuclear injection. Plasmid construction was done by Gene Bridges GmbH.

BAC DNA for pronuclear injection was prepared using NucleoBond BAC100 kit (Clontech), linearized and purified over a home-made Sepharose CL4b column. Fractions were analyzed by pulsed-field gel electrophoresis to identify the sample with the highest concentration of linearized BAC DNA and lowest concentration of vector DNA. Linearized BAC DNA was injected at a concentration of 1 ng μl^{-1} into C57BL/6 × B6C3F1 zygotes.

Transgenic mouse characterization. All experimental procedures were approved by the Institutional Animal Care and Use Committee of Allen Institute for Brain Science in accordance with US National Institutes of Health guidelines. All characterization was done using adult mice ~56 d after birth or later. The mice that were characterized were in a mixed genetic background, containing 50%–75% C57BL/6 background and the remainders of 129 or other backgrounds from the various Cre lines. For systematic characterization of fluorescent proteins either by their native fluorescence or IHC, perfused brains were cryosectioned using a tape transfer technique; sections were then DAPI stained, directly or after antibody staining, and images were captured using automated fluorescence microscopy. Microtome sections of 100-μm thickness from perfused brains were used for confocal imaging of fluorescently labeled cells. For systematic characterization of gene expression by colorimetric ISH or DFISH, we used established pipelines at the Allen Institute for tissue processing, probe hybridization, image capture and data processing. Informatics signal identification, mapping, and quantification used the Allen Mouse Brain Atlas spatial mapping platform[24,29]. In this pipeline, image series are preprocessed (white-balanced and cropped), then registered to a three-dimensional informatics reference atlas of the C57BL/6J mouse brain[28]. This registration enables data to be displayed in two-dimensional sections or reconstructed three-dimensional volumes.

Tamoxifen induction. Tamoxifen was prepared by first dissolving in ethanol (20 mg per 500 μl) and mixing this solution with 980 μl corn oil for a final concentration of 20 mg ml^{-1}. Ethanol was then removed with a heated speed vacuum. Mice containing *CreERT2* that were ~2 months old were injected with approximately 200 μl tamoxifen solution (200 mg per kilogram body weight) once a day for 5 d. They were monitored for adverse effects, and if these became apparent, treatment was stopped. One week after treatment ended, mice were processed as described below for ISH or localization of XFP.

Colorimetric *in situ* hybridization (CISH). We used systems for processing tissue, RNA ISH, Nissl staining, image acquisition, and data processing that were developed for the generation of the Allen Mouse Brain Atlas (http://mouse.brain-map.org/). The framework, workflow and equipment were previously described[24] and can be found at Data Production Processes in the Documentation – Supplementary Materials section of the Allen Mouse Brain Atlas (http://mouse.brain-map.org/pdf/ABADataProductionProcesses.pdf). Information about Cre or reporter specific probes used in ISH can be found at the Transgenic Mouse database (http://transgenicmouse.alleninstitute.org/).

Double fluorescence *in situ* hybridization (DFISH). Double fluorescence *in situ* hybridization (DFISH) was based on the CISH protocol, as described previously[44]. Briefly, riboprobes were labeled with either digoxigenin (DIG) or dinitrophenyl-11-UTP (DNP; Perkin Elmer). The DIG-labeled probe and DNP-labeled probe were hybridized simultaneously, and the signal from each was amplified with tyramide sequentially using either anti-DIG-HRP (Perkin Elmer) with tyramide-biotin or anti-DNP-HRP (Perkin Elmer) with tyramide-DNP. Signal was detected by labeling of biotin or DNP with Alexa-Fluor 488–streptavidin (Invitrogen/Molecular Probes) or Alexa Fluor 555–anti-DNP– (Invitrogen/Molecular Probes), respectively. Slides were stained on a Leica Autostainer in a 200 ng ml^{-1} solution of DAPI (Invitrogen/Molecular Probes) buffered in TNT (Tris-NaCl-Tween 20) and coverslipped with Hydromatrix mounting medium supplemented with 5.0% Dabco antifade (Sigma). Images were created from stitched tiles acquired on a DM6000B Leica microscope as described in Data Production Processes (http://mouse.brain-map.org/pdf/ABADataProductionProcesses.pdf) except that focusing and bounding boxes were established using DAPI signal.

Tape transfer sectioning. Tape transfer sectioning was done on a Leica 3050 S cryostat equipped with an Instrumedics Tape Transfer System that includes a UV light polymerization chamber and warming pad. A roll of Instrumedics tape was cut into individual flags. Slides were coated with 50 μl of Solution B adhesive and allowed to air dry. Before taking a section, slides were positioned on the warming pad. The tacky surface of the tape flag was positioned over the block face of the tissue. After a section was cut and lifted on the tape flag, it was placed on the slide on the warming pad. A brush was used to apply pressure to the tape flag so that it was thoroughly laminated to the slide. After all tape flags for a slide were laminated, the slide was placed into the UV light polymerization unit, which was subsequently activated. Following UV light treatment, the tape flags were removed with forceps, leaving the sections stuck to the slide.

Localization of XFP and immunohistochemistry. Animals were perfused with 4% paraformaldehyde in 0.1 M phosphate buffer. Brains were fixed for another 18 h at 4 °C. Brains were then cryoprotected in 20% (wt/vol) sucrose in PBS at 4 °C overnight. Brains were embedded in OCT (Tissue-Tek) and 25-μm cryosections were cut using the tape transfer method. For direct imaging of XFP, sections were DAPI-stained and coverslipped as above. For single-label immunofluorescence, sections were incubated for 30 min at 24 °C in PBS

containing 0.3% Triton X-100 (Sigma) and 5% normal goat serum (NGS). Sections were incubated with anti-GFP (Abcam; 1:1,000 dilution) overnight at 4 °C. Sections were rinsed for 30 min in PBS containing 1% NGS, incubated in Alexa Fluor 488–goat anti-rabbit IgG (Invitrogen; 1:400 dilution) for 2 h at 24 °C, rinsed for 10 min in PBS containing 1% NGS, and rinsed for 30 min in PBS. Sections were then DAPI-stained and coverslipped as above. XFP or IHC imaging was identical to the DFISH automated fluorescence microscopy method.

Confocal imaging. Perfused brains were sectioned at 100 μm using a Leica SM2000R sliding microtome. Sections were imaged using a BD CarvII spinning-disk confocal imaging system (BD Biosciences) attached to a Leica DM6000B microscope using Leica ×20/0.70 numerical aperture, ×40/1.25 numerical aperture oil or ×100/1.4 numerical aperture oil lenses as appropriate. Images were collected using a Spot Boost EM CCD camera. Images were captured with IPLab software (Scanalytics).

***In vivo* two-photon imaging.** A custom-built two-photon scanning microscope[45] with a Mai-Tai DeepSee laser (Spectra Physics) was used. Mice were anesthetized and ventilated with 0.7% isoflurane in a 20%:80% O_2:N_2 mixture and sedated using an injectable sedative, chlorprothixene (1–2 mg kg^{-1}). Through a craniotomy window, the calcium indicator dye Oregon Green BAPTA-1 (OGB) was bulk-loaded using patch pipettes into layer 2/3 of the mouse visual cortex V1[46]. Two different two-photon excitation wavelengths, 950 nm and 800 nm, were used for red tdTomato-labeled cells and the OGB signal, respectively. Images were acquired with a 605-nm filter for tdTomato and a 525-nm filter for OGB. Images were acquired at various depths (100–400 μm).

Cre-expressing recombinant adeno-associated virus (rAAV-Cre). *EGFP-Cre* (Addgene) was cloned into the pAAV-MCS vector (Stratagene). The resultant recombinant viral vector was packaged in the capsid of serotype 8, and high-titer virus (approximately 10^{13} genome copies (gc) ml^{-1}) was produced by the Harvard Gene Therapy Initiative. To visualize the projections from the somatosensory cortex, 1–2 μl of rAAV-EGFP-Cre (1.6×10^{13} gc ml^{-1}) was injected into anesthetized Ai14 mice at corresponding stereotaxic coordinates using a glass micropipette attached to a Picospritzer (Parker Hannifin). The virus was administered slowly by several low-pressure air puffs to minimize tissue damage (10 psi, 10–20 ms duration, 2 Hz and 10 min μl^{-1}). Mice then recovered and were housed individually until they were used for further analysis.

Reverse transcription–quantitative PCR of *EYFP* transcript. Tissues were dissected and immediately stored in RNALater (Ambion) at 4 °C until RNA isolation. RNA was isolated from homogenized tissues using the Trizol reagent (Invitrogen) and purified using the MagMax-96 Total RNA Isolation kit (Ambion). RNA concentration was normalized to 100 ng μl^{-1}. Equal amounts (~800 ng) of total RNA were used in each reverse transcription reaction using a Super-Script III First Strand Synthesis kit (Invitrogen) with a mixture of oligo(dT) and random primers. Each reaction was run in duplicate with reverse transcriptase (RT+) or without (RT−) to control for any potential genomic DNA contamination. Real-time quantitative PCR was conducted using cDNA (from one-twentieth of the reverse transcription reactions) with gene-specific primer pairs as well as a positive control primer pair for *Gapdh*, using SYBR Green PCR Master Mix (Roche). Each sample was run in four replicates on a Roche LightCycler Real-time PCR system. On completion of a real-time quantitative PCR experiment, the thermal denaturation profile of the resulting amplicon was determined in order to make sure that the same specific amplicon was detected in different samples. Difference in number of cycles needed to reach a threshold fluorescence with gene-specific primers as compared with *Gapdh* primers (ΔCp) was used as measure of relative mRNA abundance.

Statistical analysis. Expression levels were analyzed with two-tailed Student's *t*-test at a significance level of 0.05.

42. George, S.H. *et al.* Developmental and adult phenotyping directly from mutant embryonic stem cells. *Proc. Natl. Acad. Sci. USA* **104**, 4455–4460 (2007).
43. Zhang, Y., Buchholz, F., Muyrers, J.P. & Stewart, A.F. A new logic for DNA engineering using recombination in *Escherichia coli*. *Nat. Genet.* **20**, 123–128 (1998).
44. Thompson, C.L. *et al.* Genomic anatomy of the hippocampus. *Neuron* **60**, 1010–1021 (2008).
45. Tsai, P.S. *et al.* Principle, design and construction of a two photon laser-scanning microscope for in vitro and in vivo brain imaging. in *In Vivo Optical Imaging of Brain Function* (ed. Frostig, R.D.) 113–172 (CRC, Boca Raton, Florida, USA, 2002).
46. Garaschuk, O., Milos, R.I. & Konnerth, A. Targeted bulk-loading of fluorescent indicators for two-photon brain imaging in vivo. *Nat. Protoc.* **1**, 380–386 (2006).

doi:10.1038/nn.2467